CHEMISTRY OF MATERIALS

COMMUNICATION

pubs.acs.org/cm

Self-Assembled Amphiphilic Diketopyrrolopyrrole-Based Oligothiophenes for Field-Effect Transistors and Solar Cells

Jianguo Mei,[†] Kenneth R. Graham,[†] Romain Stalder,[†] Shree Prakash Tiwari,[‡] Hyeunseok Cheun,[‡] Jaewon Shim,[‡] Masafumi Yoshio,[§] Colin Nuckolls,[§] Bernard Kippelen,[‡] Ronald K. Castellano,[†] and John R. Reynolds*[,†]

[†]The George and Josephine Butler Polymer Research Laboratory, Department of Chemistry, University of Florida, Gainesville, Florida 32611, United States

[‡]School of Electrical and Computer Engineering, Georgia Institute of Technology, Atlanta, Georgia 30332, United States

[§]Department of Chemistry, Columbia University, New York, New York 10027, United States

Supporting Information

KEYWORDS: amphiphile, diketopyrrolopyrrole, field-effect transistor, oligothiophene, self-assembly, solar cell

Diketopyrrolopyrrole-based (DPP) conjugated molecules and polymers are gaining attention as active materials in field-effect transistors and organic solar cells.[1] Recent examples include DPP-based polymers with balanced hole and electron mobilities (0.1 $cm^2 V^{-1} s^{-1}$ and 0.09 $cm^2 V^{-1} s^{-1}$, respectively) in solution-processed ambipolar field-effect transistors (FETs)[1a] and DPP-based "transistor paint" that displays reproducible mobility values of 0.28 $cm^2 V^{-1} s^{-1}$.[1g] Larger hole mobilities (up to 1.95 $cm^2 V^{-1} s^{-1}$) have been reported for a DPP and thieno-[3,2-*b*]thiophene containing copolymer in an FET.[1h,m] Equally exciting, DPP-containing polymers show promise as electron donor materials in bulk-heterojunction solar cells.[1c−f,m] Janssen et al. recently reported power conversion efficiencies (PCEs) of up to 5.5% for dithieno-DPP-phenylene copolymers blended with fullerene acceptors.[1f] Particularly relevant to the current work, DPP-based small molecules are also yielding promising results for organic photovoltaics.[1i−l] Exemplary is the work of Nguyen et al. that has demonstrated PCEs of 2.2−4.4% for solution-processed DPP-core oligomers, findings that have stimulated others to identify other unique "cores" for *molecular* heterojunction solar cells.[2]

The self-assembly of organic molecules into supramolecular structures[3] holds promise for efforts that seek to control solid-state morphology and optimize optoelectronic device performance. In this context, a reliable and widely used molecular design strategy involves the introduction of amphiphilic character to a molecular scaffold to promote noncovalent assembly formation.[3b−d] Here we show how extension of the amphiphilic molecular design to a DPP-based π-conjugated oligomer confers a rich self-assembly profile in solution and the bulk and explore how the amphiphilic material behaves in field-effect transistor and solar cell devices.

The molecule designed for this study (DPP_{amphi}) features a diketopyrrolopyrrole (DPP) oligothiophene core, along with terminal lipophilic paraffinic chains and lateral hydrophilic triglyme chains (Figure 1a,b). The extended and rigid conjugated DPP core ensures strong $\pi-\pi$ interactions,[4] while orthogonally placed hydrophilic triglyme and hydrophobic paraffinic chains provide, at the outset, desirable processing solubility for device fabrication. Indeed, control studies have found that the solubility of the molecule in organic solvents drops dramatically upon replacing the triglyme chains with dodecyl ($C_{12}H_{25}$) chains.

The synthesis of DPP_{amphi} involves an efficient Stille coupling between the dibrominated DPP core and stanylated bithiophene wings (see Supporting Information). Differential scanning calorimetry (DSC), polarized light microscopy, and X-ray diffraction reveal the rich phase behavior accessible to DPP_{amphi}. DSC (Figure 1c at 5 °C/min) upon heating shows an endothermic transition at 68 °C (12.4 kJ/mol), followed by a second transition at 98 °C (25.2 kJ/mol), and finally a clearing point at 184 °C (33.0 kJ/mol). Upon cooling, three corresponding exothermic transitions are observed at 181, 92, and 65 °C with enthalpies of 32.8, 22.2, and 17.7 kJ/mol, respectively. After the second scan, subsequent scans reproducibly overlap the prior scan. In order to gain insight for later solar cell studies, a blend of DPP_{amphi} and $PC_{60}BM$ was investigated under the same conditions. Although a lower crystallization temperature (154 °C) is observed upon cooling (Figure S1, Supporting Information), the DSC thermogram exhibits a similar profile to the neat material indicating that the corresponding phases are largely preserved.

Upon cooling the neat sample from the isotropic melt and shearing at 170 °C, a highly ordered, birefringent palm-tree-leaf-like texture emerges by polarized light microscopy (Figure 1d). Its appearance (i.e., domain size and color) and pseudouniaxial solid phase growth can be controlled. Snapshots of the directed growth that accompanies external shearing are presented in Supporting Information Figure S2, where images have been taken every five seconds. Noticeably, while the fluidity of DPP_{amphi} is largely reduced after shearing, the material still appears to be soft and waxy. Given its texture, the mesophase seems more consistent with a columnar plastic phase than a liquid-crystalline phase (vide infra).[5] Another phase change, possibly from a less ordered to a more ordered columnar plastic crystal phase, is subsequently observed around

Received: January 3, 2011
Revised: March 23, 2011
Published: April 12, 2011

dx.doi.org/10.1021/cm1036869 | *Chem. Mater.* 2011, 23, 2285–2288

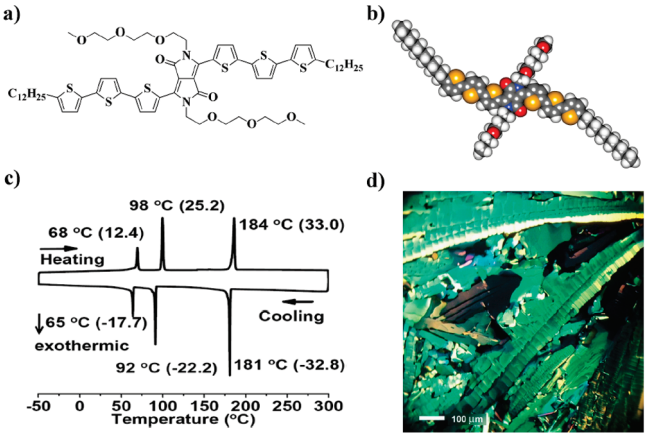

Figure 1. (a) DPP_{amphi} molecular structure, (b) DFT-optimized geometry (B3LYP/6-31G*) as a space-filling model (atom color code: C = gray; N = blue; O = red; S = yellow; H = white), (c) differential scanning calorimetry (DSC) thermogram (enthalpy values are reported in parentheses in kJ mol^{-1}), and (d) polarized light microscopy image of DPP_{amphi} at 170 °C (after shearing).

90 °C, in good agreement with the DSC results, and may correspond to crystallization of the two terminal alkyl chains. With the formation of another crystalline phase below 65 °C, possibly associated with solidification of the flexible triglyme chains, a mosaic-like appearance is observed (Supporting Information Figure S3). The crystal phase behavior, which is significantly different from that reported for Nguyen's all-alkyl-substituted DPP molecules, presumably arises from the amphiphilic character of DPP_{amphi}.[1k]

Variable temperature X-ray diffraction patterns of DPP_{amphi} obtained at 170, 80, and 50 °C (temperatures corresponding to the phases reported by DSC) upon cooling from the isotropic melt are shown in Supporting Information Figure S4. Sharp Bragg reflections accompany both high temperature mesophases (170 and 80 °C), consistent with long-range ordering and the assignment of plastic phases. That the substance is shearable at temperatures close to the clearing temperature and bears a rather soft and waxy texture excludes the possibility that a true crystalline phase exists at 170 °C. By the same argument, DPP_{amphi} is likely not a plastic crystal below 65 °C given that the texture is not deformable. The assignment of the mesophase at 80 °C remains tentative as it is generally (due to the orientational disorder) not insightful to index the reflection peaks for plastic crystal phases by one-dimensional X-ray diffraction.[6]

After establishing the phase behavior of DPP_{amphi} in the bulk, its self-association behavior was explored in solution and on surfaces. UV−vis spectra of DPP_{amphi} in methylcyclohexane (MCH) were recorded every 45 s at 30 °C, after initial equilibration at 60 °C. Figure 2a shows the growth of a broad absorption with $\lambda_{max} \sim 750$ nm (and color change from blue to purple), indicating the existence of strong excitonic interactions and the formation of π-stacks. The isosbestic point at 680 nm further demonstrates a stoichiometric conversion from free molecules to crystals (aggregates). Strong $\pi-\pi$ stacking typically leads to a nonemitting crystal phase, due to the forbidden low-excitonic transition.[7] This is consistent with fluorescence measurements; DPP_{amphi} is emissive in a good solvent as a dilute solution, but no emission is detected in thin films.

In order to "visualize" the consequences of aggregation, the system was studied by atomic force microscopy (AFM) on a surface.

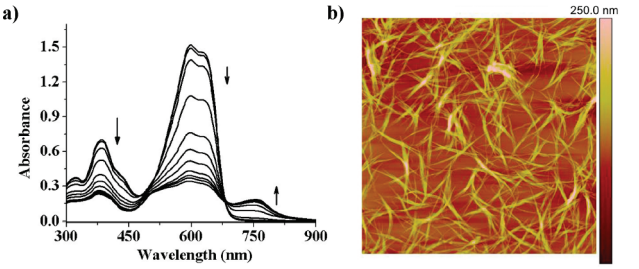

Figure 2. (a) UV−vis spectra of DPP_{amphi} in methylcyclohexane (2.2×10^{-5} M, at 30 °C) recorded at 45 s intervals; (b) tapping mode AFM image (20×20 μm) of DPP_{amphi} as deposited from THF−hexanes onto mica.

When a 2.2×10^{-4} M solution of DPP_{amphi} in THF, a good solvent, is added dropwise to hexane, a poor solvent, the solution turns from blue to purple, indicating the formation of aggregates. Deposition of the suspension on mica reveals uniform nanoscale fiber-like assemblies (Figure 2b). Similar aggregates also form when a solution of DPP_{amphi} in methylcyclohexane (MCH) is heated and allowed to cool to room temperature. These solution studies demonstrate that DPP_{amphi} has a strong tendency to self-assemble into highly ordered nanofibrils, most likely through synergistic solvophobic effects and $\pi-\pi$ interactions.

To investigate the effect of self-organization of DPP_{amphi} at the interface between solution and substrate, a process relevant to the fabrication of an organic electronic device in which solution-processing and a high degree of ordering are both desired, DPP_{amphi} chlorobenzene solutions (2.2×10^{-4} M) were drop-cast onto the surface of freshly cleaved mica and studied by AFM. Tapping mode AFM images and line traces in Figure 3 show a significant increase in ordering in three samples as the solvent evaporation time is increased from 3.5 to 8.5 min. At 3.5 min, irregular aggregates have formed based on the height fluctuation of the line trace across the surface. At 5 min, sharper features with even steps in height of 3.6−4.0 nm have developed, a much more ordered arrangement. At an evaporation time of 8.5 min, the molecules have assembled into larger, belt-like domains with uniform step height of 3.6−4.0 nm. Proposed is that the step-height of 3.6−4.0 nm corresponds to DPP_{amphi} molecules that are packed with their long axes oriented perpendicular to the substrate.

To determine whether the proclivity of DPP_{amphi} to form π-stacks via self-assembly has a pronounced impact on device performance, top contact field-effect devices with gold top source/drain electrodes and DPP_{amphi} as the organic semiconductor were spin-cast from chlorobenzene on O_2 plasma cleaned bare SiO_2. Figure 4 shows the output and transfer characteristics of a particular p-channel OFET (W/L = 1200 μm/25 μm) with DPP_{amphi} after annealing at 130 °C for 30 min. The operating voltage for the devices is −60 V. The OFETs exhibited average hole mobility values of 3.4×10^{-3} $cm^2V^{-1}s^{-1}$ and current on/off ratios of 1×10^4, with the average threshold voltage of 6.4 V (more details are given in Table S1, Supporting Information). The results are comparable to previously reported DPP molecules (where mobilities of $4-9 \times 10^{-3}$ $cm^2V^{-1}s^{-1}$; were obtained)[1k] and suggest that introduction of flexible triglyme chains does not necessarily depreciate the device performance, but it does impart desirable solubility for purification and processing.

Solution-processed molecular bulk-heterojunction solar cells were subsequently fabricated using DPP_{amphi} as an electron donor

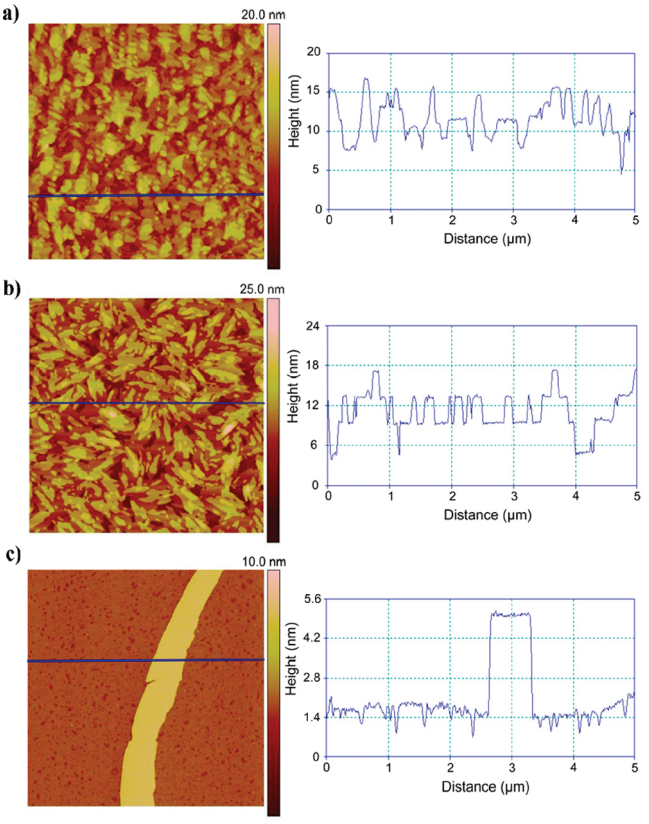

Figure 3. Tapping mode AFM images (5 × 5 μm) with z-height line scan profiles of DPP_{amphi} drop-cast from chlorobenzene (2.2×10^{-4} M) on mica. Solvent evaporation times are (a) 3.5, (b) 5, and (c) 8.5 min. Scale bars are different in parts a, b, and c, and each step is about 3.6−4.0 nm.

material and $PC_{60}BM$ as an electron acceptor material in an ITO/PEDOT:PSS/DPP_{amphi}:$PC_{60}BM$/Al device. The LUMO and HOMO levels of DPP_{amphi}, −3.9 and −5.5 eV, respectively, together with an energy gap of 1.6 eV, were obtained by electrochemistry (Supporting Information Figure S5). The current−voltage characteristics of a representative device before and after annealing are shown in Supporting Information Figure S6. Devices with an active layer thickness of ∼100 nm yielded a short circuit current density (J_{sc}) of 1.56 ± 0.06 mA/cm^2, an open circuit voltage (V_{oc}) of 0.50 ± 0.01 V, a fill factor (FF) of 0.54 ± 0.01, and a power conversion efficiency of 0.43 ± 0.01% under AM 1.5 G, 100 mW/cm^2 illumination (averaged from five devices). Upon annealing at 90 °C, the devices exhibited an enhanced J_{sc} of 2.41 ± 0.07 mA/cm^2, a V_{oc} of 0.55 ± 0.02 V, a FF of 0.55 ± 0.03, and a power conversion efficiency of 0.68 ± 0.02%. The external quantum efficiency increased upon annealing from 10% to above 15% in the 415−580 nm and 620−770 nm range. The PCEs of these minimally optimized devices are lower than the state-of-the-art solution-processed molecular BHJ solar cells, likely due to undesirable phase separation. However, the *fill factors* of the devices before and after annealing are higher than the large majority of other solution-processed molecular solar cells reported in the literature[8] and comparable to those of the best performing vacuum-deposited molecular heterojunction solar cells.

In summary, we have demonstrated the design, synthesis, and characterization of an amphiphilic π-conjugated low energy gap oligomer, DPP_{amphi}. We are exploring whether the same design

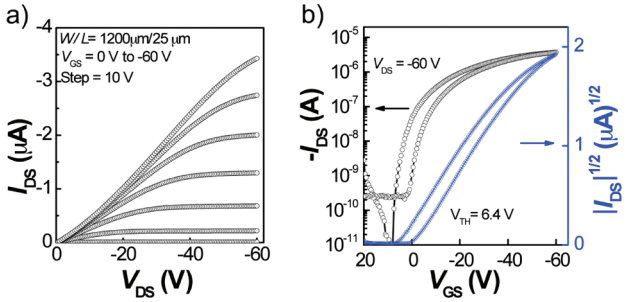

Figure 4. (a) Output and (b) transfer characteristics of a representative DPP_{amphi} field-effect transistor device.

principles used to achieve desirable solution processability and long-range order via self-assembly with DPP_{amphi} can be extended to other semiconductor scaffolds considered attractive as active materials in field-effect transistor and photovoltaic devices.

■ ASSOCIATED CONTENT

Ⓢ Supporting Information. Synthesis, characterization, and device fabrication details (PDF, AVI). This material is available free of charge via Internet at http://pubs.acs.org.

■ ACKNOWLEDGMENT

We gratefully acknowledge the AFOSR (FA9550-09-1-0320) and the STC program of the NSF (DMR-0120967) for financial support.

■ REFERENCES

(1) (a) Bürgi, L.; Turbiez, M.; Pfeiffer, R.; Bienewald, F.; Kirner, H. J.; Winnewisser, C. *Adv. Mater.* **2008**, *20*, 2217–2224. (b) Wienk, M. M.; Turbiez, M.; Gilot, J.; Janssen, R. A. J. *Adv. Mater.* **2008**, *20*, 2556–2560. (c) Bijleveld, J. C.; Zoombelt, A. P.; Mathijssen, S. G. J.; Wienk, M. M.; Turbiez, M.; de Leeuw, D. M.; Janssen, R. A. J. *J. Am. Chem. Soc.* **2009**, *131*, 16616–16617. (d) Zhou, E.; Yamakawa, S.; Tajima, K.; Yang, C.; Hashimoto, K. *Chem. Mater.* **2009**, *21*, 4055–4061. (e) Huo, L.; Hou, J.; Chen, H.-Y.; Zhang, S.; Jiang, Y.; Chen, T. L.; Yang, Y. *Macromolecules* **2009**, *42*, 6564–6571. (f) Bijleveld, J. C.; Gevaerts, V. S.; Di Nuzzo, D.; Turbiez, M.; Mathijssen, S. G. J.; de Leeuw, D. M.; Wienk, M. M.; Janssen, R. A. J. *Adv. Mater.* **2010**, *22*, E242–E246. (g) Nelson, T. L.; Young, T. M.; Liu, J.; Mishra, S. P.; Belot, J. A.; Balliet, C. L.; Javier, A. E.; Kowalewski, T.; McCullough, R. D. *Adv. Mater.* **2010**, *22*, 4617–4621. (h) Li, Y.; Singh, S. P.; Sonar, P. *Adv. Mater.* **2010**, *22*, 4862–4866. (i) Tamayo, A. B.; Walker, B.; Nguyen, T.-Q. *J. Phys. Chem. C* **2008**, *112*, 11545–11551. (j) Walker, B.; Tamayo, A. B.; Dang, X. D.; Zalar, P.; Seo, J. H.; Garcia, A.; Tantiwiwat, M.; Nguyen, T.-Q. *Adv. Funct. Mater.* **2009**, *19*, 3063–3069. (k) Tantiwiwat, M.; Tamayo, A.; Luu, N.; Dang, X.-D.; Nguyen, T.-Q. *J. Phys. Chem. C* **2008**, *112*, 17402–17407. (l) Tamayo, A. B.; Dang, X.-D.; Walker, B.; Seo, J.; Kent, T.; Nguyen, T.-Q. *Appl. Phys. Lett.* **2009**, *94*, 103301. (m) Bronstein, H.; Chen, Z.; Ashraf, R. S.; Zhang, W.; Du, J.; Durrant, J. R.; Tuladhar, P. S.; Song, K.; Watkins, S. E.; Geerts, Y.; Wienk, M. M.; Janssen, R. A. J.; Anthopoulos, T.; Sirringhaus, H.; Heeney, M.; McCulloch, I. *J. Am. Chem. Soc.* **2011**, *133*, 3272–3275.

(2) Mei, J.; Graham, K. R.; Stalder, R.; Reynolds, J. R. *Org. Lett.* **2010**, *12*, 660–663. (b) Rousseau, T.; Cravino, A.; Ripaud, E.; Leriche, P.; Rihn, S.; De Nicola, A.; Ziessel, R.; Roncali, J. *Chem. Commun.* **2010**, *46*, 5082–5084.

(3) (a) Yamamoto, Y.; Fukushima, T.; Suna, Y.; Ishii, N.; Saeki, A.; Seki, S.; Tagawa, S.; Taniguchi, M.; Kawai, T.; Aida, T. *Science* **2006**, *314*, 1761–1764. (b) Zhang, X; Chen, Z; Würthner, F. *J. Am. Chem. Soc.* **2007**, *129*, 4886–4887. (c) Li, W; Yamamoto, Y; Fukushima, T;

Saeki, A; Seki, S; Tagawa, T; Masunaga, H; Sasaki, S; Takata, M; Aida, T. *J. Am. Chem. Soc.* **2008**, *130*, 8886–8887. (d) Feng, X.; Marcon, V.; Pisula, W.; Hansen, M. R.; Kirkpatrick, J.; Grozema, F.; Andrienko, D.; Kremer, K.; Müllen, K. *Nat. Mater.* **2009**, *8*, 421–426.

(4) (a) Song, B.; Wei, H.; Wang, Z.; Zhang, X.; Smet, M.; Dehaen, W. *Adv. Mater.* **2007**, *19*, 416–420. (b) Song, B.; Wang, Z.; Chen, S.; Zhang, X.; Fu, Y.; Smet, M.; Dehaen, W. *Angew. Chem., Int. Ed.* **2005**, *44*, 4731–4735.

(5) (a) Bushey, M. L.; Hwang, A.; Stephens, P. W.; Nuckolls, C. *J. Am. Chem. Soc.* **2001**, *123*, 8157–8158. (b) Li, J. L.; Kastler, M.; Pisula, W.; Robertson, J. W. F.; Wasserfallen, D.; Grimsdale, A. C.; Wu, J. S.; Müllen, K. *Adv. Funct. Mater.* **2007**, *17*, 2528–2533. (c) Pisula, W.; Kastler, M.; Wasserfallen, D.; Mondeshki, M.; Piris, J.; Schnell, I.; Müllen, K. *Chem. Mater.* **2006**, *18*, 3634–3640. (d) Simmerer, J.; Glüsen, B.; Paulus, W.; Kettner, A.; Schuhmacher, P.; Adam, D.; Etzbach, K.-H.; Siemensmeyer, K.; Wendorff, J. H.; Ringsdorf, H.; Haarer, D. *Adv. Mater.* **1996**, *8*, 815–819.

(6) Boden, N.; Bushby, R. J.; Lozman, O. R.; Lu, Z. B.; McNeill, A.; Movaghar, B. *Mol. Cryst. Liq. Cryst.* **2004**, *410*, 541–549.

(7) Balakrishnan, K.; Datar, A.; Oitker, R.; Chen, H.; Zuo, J.; Zang, L. *J. Am. Chem. Soc.* **2005**, *127*, 10496–10497.

(8) Bagnis, D.; Beverina, L.; Huang, H.; Silvestri, F.; Yao, Y.; Yan, H.; Pagani, G. A.; Marks, T. J.; Facchetti, A. *J. Am. Chem. Soc.* **2010**, *132*, 4074–4075. (b) Roncali, J. *Acc. Chem. Res.* **2009**, *42*, 1719–1730. (c) Walker, B.; Kim, C.; Nguyen, T.-Q. *Chem. Mater.* **2011**, *23*, 470–482.